Optical rogue waves in coupled fiber Raman lasers

S. KOLPAKOV, [1] S. V. SERGEYEV,[1,*] A. UDALCOVS,[2] X. PANG,[2,3] O. OZOLINS, [2,3] R. SCHATZ[2] AND S. POPOV[2]

[1]*Aston Institute of Photonics Technologies, Aston University, Birmingham, B4 7ET, UK*
[2]*KTH Royal Institute of Technology, Isafjordsgatan 22, 164 40 Kista, Sweden*
[3]*RISE Research Institutes of Sweden, Isafjordsgatan 22, 164 40 Kista, Sweden*
**Corresponding author: s.sergeyev@aston.ac.uk*

Received XX Month XXXX; revised XX Month, XXXX; accepted XX Month XXXX; posted XX Month XXXX (Doc. ID XXXXX); published XX Month XXXX

For coupled linear cavity-random fiber Raman lasers, for the first time, we demonstrate a new mechanism of emergence of the random pulses with the anomalous statistics satisfying optical rogue waves' criteria experimentally. The rogue waves appear as a result of the coupling of two Raman cascades, namely, a linear cavity laser with a wavelength of 1.55 μm and a random laser with wavelengths nearby 1.67 μm, along with coupling of the orthogonal states of polarization (SOPs). The coherent coupling of SOPs causes localization of the trajectories in the vicinity of these states, whereas polarization instability drives escape taking the form of chaotic oscillations. Antiphase dynamics in two cascades results in the suppression of low amplitude chaotic oscillations and enabling the anomalous spikes satisfying rogue waves criteria. © 2020 Optical Society of America

http://dx.doi.org/10.1364/OL.99.099999

For the last two decades, the study of the statistics and mechanisms of origin waves with anomalous amplitude (rogue waves, RWs) have been in the focus of research in different fields ranging from oceanography to the laser physics [1-16]. This study aims to find approaches for predicting and mitigating the RWs' emergence . For the classification of rare events with an anomalous amplitude as the RWs, the following criteria have been suggested: (i) RWs should have amplitude exceeding the standard deviation of waves' amplitude σ in more than eight times; (ii) tails of probability distribution density for RWs' amplitudes have to deviate significantly from Gaussian or Rayleigh distributions [1].

Fiber lasers provide a unique opportunity to collect more data on optical rogue waves for a short time in a controllable laboratory environment. For example, the mechanisms of optical RWs emergence have been already revealed both experimentally and theoretically in mode-locked fiber lasers [1-12], Raman fiber lasers with different resonators, and without resonators (random lasers) [13-19], along with lasers with the randomly distributed fiber Bragg gratings (FBGs) [20].

One of such mechanisms – polarization instability (PI) – has been found in erbium-doped mode-locked fiber lasers [3-5, 10-12]. The observed PI leads to the phase difference slip between orthogonal states of polarization (SOPs) of the laser optical wave and contributes to the formation of the RWs in the form of chaotic pulse bunching (soliton rain), as well as fundamental and second-order Akhmediev breathers- and Peregrine solitons – like spatio-temporal structures [3-5, 10-12]. This scenario is similar to the RWs mechanism found for the dynamics of coupled nonlinear oscillators where desynchronization causes random relative phase slips leading to the appearance of rogue waves [21].

In this Letter, we provide results on an experimental study of synchronization scenario of the coupled oscillators by using a testbed system, namely coupled fiber Raman laser cascades – a linear cavity with 1.55 μm wavelength and a random laser with the wavelength of 1.67 μm – emitting light at two orthogonal linearly polarized SOPs. We have found that the interplay of the PI with the antiphase dynamics of the 1.55 μm and 1.67 μm cascades leads to the emergence of anomalous power spikes with the RWs statistics.

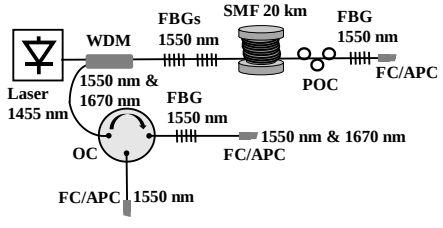

Fig. 1 Linear cavity and random fiber Raman lasers.

The schematic sketch of the fiber Raman laser is shown in Fig. 1. The set-up comprises of 20 km of an SMF fiber, fiber

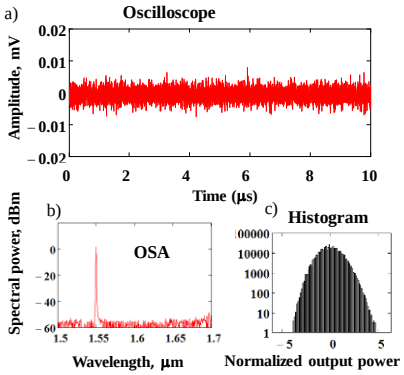

Fig. 2 Fast dynamics at the 1.55 μm: a) oscilloscope trace for *P=35 dBm*, b) optical spectrum, c) histogram of the output power distribution, output voltage V is normalized to standard deviation σ as $V_n=(V-mean(V))/\sigma(V)$.

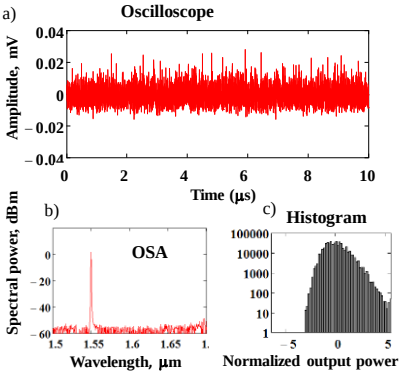

Fig. 4 Fast dynamics at the 1.55 μm & 1.67 μm for *P=35 dBm*: a) oscilloscope trace, b) optical spectrum, c) histogram of the output power distribution. Output power voltage in oscilloscope is normalized as shown in Fig. 2.

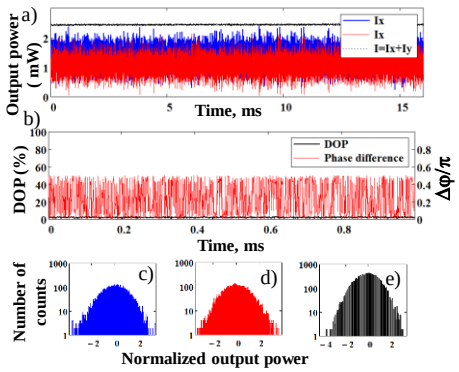

Fig. 3. Slow dynamics at 1.55 μm for P=35 dBm: (1 μs resolution, 16 slices with 1024 points per slice): a) the output power vs time: I_x (blue), I_y (red) and $I=I_x+I_y$ (black); b) the phase differences (red) and *DOP* (black) vs time; c)–e) Probability distribution histograms for the output power I_x (c), I_y (d), and total output power $I=I_x+I_y$ (e). Each output power I_i (I, I_x, I_y) is normalized as shown in Fig. 2.

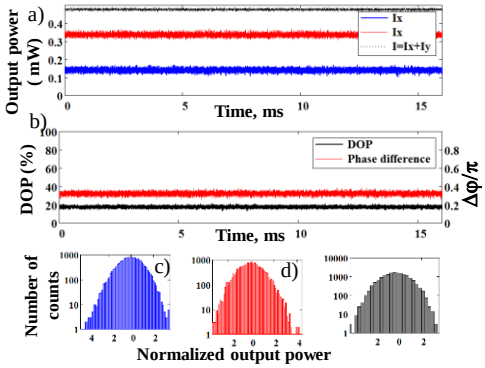

Fig. 5. Slow dynamics at 1.55 μm & 1.67 μm for *P=35 dBm*: (1 μs resolution, 16 slices with 1024 points per slice): a) the output power vs time: I_x (blue), I_y (red) and $I=I_x+I_y$ (black); b) the phase differences (red) and *DOP* (black) vs time; c)–e) Probability distribution histograms for the output power I_x (c), I_y (d), and total output power $I=I_x+I_y$ (e). Each output power I_i (I, I_x, I_y) is normalized as shown in Fig. 2.

Bragg gratings (FBGs) (the central wavelength λ_c=1550 nm,reflection coefficient r=90%, bandwidth $\Delta\lambda_{FWHM}$=0.5 nm), and polarization controller (POC). To enable the second cascade (1670 nm) random lasing, we use FC/APC connector to suppress back reflection. The cavity was pumped via a 1455/1550 nm WDM by using a 1455 nm fiber laser (Keopsys CRFL, 5 W maximum power). The lasing signal was split into two channels (1550 nm and 1550 nm & 1670 nm) by using optical circulator (OC) and FBG. The lasing signal at the fast time scale (2 ns – 1ms) was measured in both channels by using photodetectors with a bandwidth of 10 GHz (ORTEL 2860-CO1) connected to a 500 MHz sampling oscilloscope (Tektronix TDS 754A). There were collected 500K samples to build a histogram of the output power distribution. Since each output voltage V is normalized to standard deviation σ as

V_n=(V-mean(V))/σ(V), the RW criterion looks as $V_n > 8$. An in-line polarimeter (Thorlabs IPM5300) was used to record the state and degree of polarization (SOP and DOP), respectively. To reveal the RW emergence at the slow time scales of 1 μs – 16 ms, we used polarimeter to record 16 traces with 1024 samples in each and 1 μs sample interval. As a result, we found the degree of polarization (DOP), output power and normalized Stokes parameters s_1, s_2, s_3 which are related to the output power of two linearly cross-polarized SOPs I_x and I_y, and the phase difference between them Δϕ as follows:

$$S_0 = I_x + I_y, \quad S_1 = I_x - I_y, \quad S_2 = 2\sqrt{I_x I_y}cos(\Delta\varphi),$$

$$S_3 = 2\sqrt{I_x I_y}sin(\Delta\varphi), s_i = \frac{S_i}{\sqrt{S_1^2 + S_2^2 + S_3^2}},$$

$$DOP = \frac{\sqrt{S_1^2+S_2^2+S_3^2}}{S_0}, \ (i = 1,2,3). \qquad (1)$$

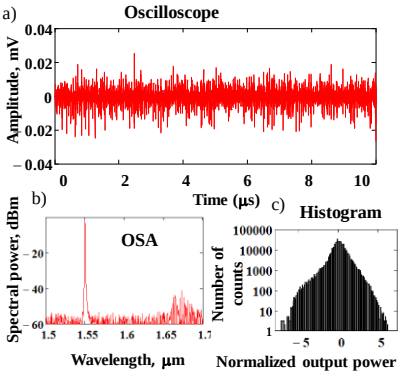

Fig. 6 Fast dynamics at the 1.55 μm for *P=37 dBm*: a) oscilloscope trace, b) optical spectrum, c) histogram of the output power distribution. Output power voltage in oscilloscope is normalized as shown in Fig. 2.

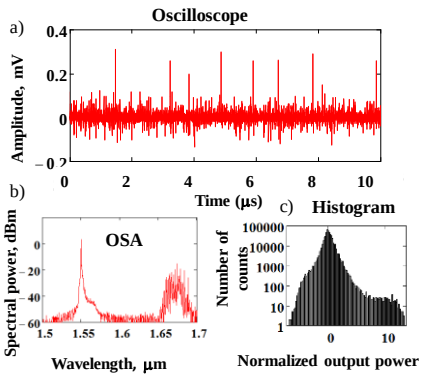

Fig. 8. Fast dynamics at the 1.55 μm & 1.67 μm for P=37 dBm: a) oscilloscope trace, b) optical spectrum, c) histogram of the output power distribution. Output power voltage in oscilloscope is normalized as shown in Fig. 2.

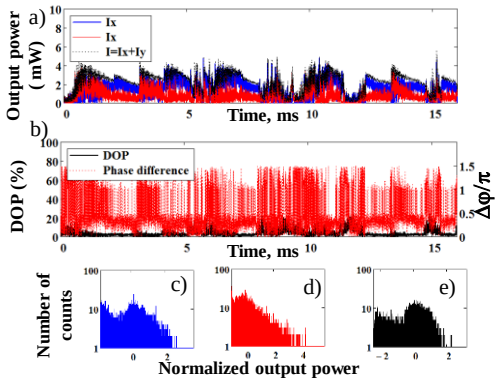

Fig. 7. Slow dynamics at 1.55 μm for *P=37 dBm* (1 μs resolution, 16 slices with 1024 points per slice): a) the output power vs time: I_x (blue), I_y (red) and $I=I_x+I_y$ (black); b) the phase differences (red) and DOP (black) vs time; c)–e) Probability distribution histograms for the output power I_x (c), I_y (d), and total output power $I=I_x+I_y$ (e). Each output power I_i (I, I_x, I_y) is normalized as shown in Fig. 2.

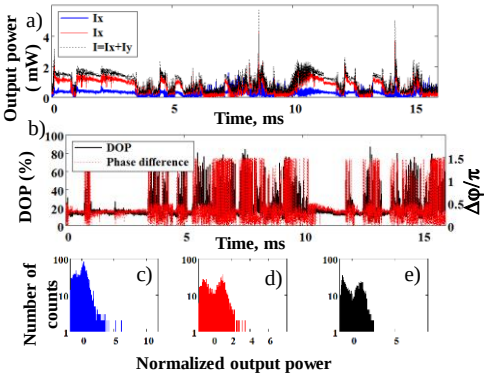

Fig. 9. Slow dynamics at 1.55 μm & 1.67 μm for the pump power *P=37 dBm* (1 μs resolution, 16 slices with 1024 points per slice): a) the output power vs time: I_x (blue), I_y (red) and $I=I_x+I_y$ (black); b) the phase differences (red) and *DOP* (black) vs time; c)–e) Probability distribution histograms for the output power I_x (c), I_y (d), and total output power $I=I_x+I_y$ (e). Each output power I_i (I, I_x, I_y) is normalized as is shown in Fig. 2.

The results for the pump power of *P=35 dBm* and *P=37 dBm*, and fast and slow dynamics for the filtered channels 1.55 μm and 1.55 μm & 1.67 μm, are shown in Figs. 2-9.

The fast (2 ns – 10 μs) and slow (1 μs -16 ms) dynamics for the case of the filtered 1.55 μm channel and the pump power of 35 dBm is shown in Fig. 2 and 3. As follows from Fig. 2, pump power *P=35 dBm* corresponds to the power near the threshold of the random lasing at 1.67 μm (Fig. 2 (b)). As follows from the set-up configuration in Fig.1, though the output signal is attenuated to the low level, the output dynamics in Fig. 2 (a) is affected by the detected bandwidth limitation of the oscilloscope [16]. As a result, the instrumental impact leads to the histogram deformation and so the output power statistics is close to the Gaussian one (Fig. 2 (c)) [16].

The slow dynamics shown in Fig. 3 (a, b) reveals the polarization instability and antiphase dynamics of the output power for horizontally- (x-component) and vertically- (y- component)-polarized modes. Low DOP of 2 % indicates that polarization dynamics is fast, and it takes the form of switching between orthogonally polarized SOPs caused by the polarization instabilities [17, 18]. As we demonstrate further, the presence of the second cascade random Raman laser at 1.67 μm results in the skewed histogram, and, so, for the case shown in Figs. 3 (c-d) the output power statistics is symmetrical and close to the Gaussian one.

The fast and slow dynamics for the case of the 1.55 μm & 1.67 μm channel, and the pump power of 35 dBm, is shown in Fig. 4 and 5. As follows from Fig.4 (a-c), the output dynamics in Fig. 4 (a) is effected by the amplified spontaneous emission at 1.67 μm, in addition to the dynamic instabilities and photodetector noise. As a result, the output power statistics is skewed (Fig. 4 (c)).

The slow dynamics shown in Fig. 5 (a, b) reveals the antiphase dynamics of the output 1.55 μm & 1.67 μm. Increased DOP from 2 % to 20 % indicates that polarization dynamics is fast, and it takes the form of antiphase dynamics for each polarization mode at 1.55 μm and 1.67 μm wavelengths. As we demonstrate further, the presence of the second cascade random Raman lasing at 1.67 μm results in the skewed histogram, and, so, since the output is close to the threshold of the random lasing, the output power statistics is symmetrical (Fig. 5 (c-e)). The locked state of polarization and *DOP=20%* indicates that polarization dynamics is fast, and the real polarization attractor has a different form [10].

With the increase of the pump power to 37 dBm, the fast and slow dynamics is affected by the random lasing at 1.67 μm as shown in Figs. 6-9.

For 1.55 μm, the fast dynamics is shown in Fig.6 (a-c). The maximum of the spectral power of the random lasing is attenuated by 40 dB with respect to the maximum of the 1.55 μm spectral power (Fig.6 (b)). The dynamics is shown in Fig. 6 (a) is slightly affected by the attenuated lasing at 1.67 μm, and, so, the power distribution is skewed.

The slow dynamics is shown in Fig. 7 (a-e). As follows from Fig. 7 (a-b), the polarization instability takes the form of the phase difference slips in π that leads to the spike in output power for x and y components and the total power. As follows from Eq. 1, the low DOP is a result of the fast oscillations of the SOP with Stokes parameters changing sign. Though the polarization instability leads to the skewed distribution of the output power, this distribution has no tail with normalized power $V_n>8$.

Unlike the previous case, output power at the mixed channel 1.55 μm & 1.67 μm has fast dynamics with rare spikes as shown in Fig. 8 (a). Increased spectral power at 1.67 μm (Fig. 8 (b)) leads to the antiphase dynamics at 1.55 μm and 1.67 μm that results in cleansing the oscillogram at the mixed channel and, so, to a distribution satisfying the rogue waves statistics (Fig. 8 (c)).

The slow dynamics is shown in Fig. 9 (a-e). As follows from Fig. 9 (a-b), the polarization instability and antiphase dynamics at 1.55 μm & 1.67 μm results in rare phase difference slips and, so, in rare spikes in output power for x and y components and the total power. As follows from Eq. 1, the increased DOP is a result of the suppression of the fast oscillations of the SOP. As a result of the antiphase dynamics, rare spikes have the power distribution satisfying the RW statistics for x component (Figs. 9 (c-e)), i.e. it has a tail with normalized power $V_n>8$.

In conclusion, we demonstrated the fast and slow dynamics in the system of coupled 20 km linear cavity–random fiber Raman lasers. We found that the antiphase dynamics of the output power for the lasing at 1.55 μm (linear cavity laser) and 1.67 μm (random laser) leads to the suppression of the fast oscillations. The polarization instability in the form of the phase difference slips in π results in the emergence of spikes in output power for x and y components, and the total power too. As a result, the statistics of spikes can satisfy the rogue wave's criteria.

Funding. FP7-PEOPLE-2012-IAPP (project GRIFFON, No. 324391), Leverhulme Trust (Grant ref: RPG-2014-304), Swedish Research Council (VR) Starting Grants No. 2019-05197 and No. 2016-04510 and the Swedish Innovation Agency (VINNOVA)-funded project "Centre for Software-Defined Optical Networks (No. 2017-01559)".

Disclosures. The authors declare no conflicts of interest.

References

1. M. Onorato, S. Residori, U. Bortolozzo, A. Montina, and F. T. Arecchi, Phys. Rep. **528**, 47 (2013).
2. N. Akhmediev, B. Kibler, F. Baronio, M. Belić, W. P. Zhong, Y. Zhang, et al. J Optics **18**, 063001 (2016).
3. H. Kbashi, S. V. Sergeyev, C. Mou, C., A. Martinez, M. A. Araimi, A. Rozhin, et al. Ann. Phys. **530**, 1700362. (2018).
4. H. J. Kbashi, S. V. Sergeyev, M. A. Araimi, N. Tarasov, N. and A. Rozhin, A., Laser Phys. Lett. **16**, 035103 (2019).
5. H. J. Kbashi, M. Zajnulina, A. G. Martinez, S. V. Sergeyev, Laser Phys. Lett. **17**, 035103 (2020).
6. J. M. Dudley, F. Dias, M. Erkintalo, and G. Genty, Nature Photon. **8,** 755-764 (2014)
7. C. Lecaplain, Ph. Grelu, J. M. Soto-Crespo, and N. Akhmediev, J. Opt. 15, 064005 (2013).
8. C. Lecaplain, Ph. Grelu, J. M. Soto-Crespo and N. Akhmediev, Phys. Rev. Lett. **108**, 233901 (2012).
9. J. M. Soto-Crespo, Ph. Grelu, and N. Akhmediev, Phys. Rev. E **84**, 016604 (2011).
10. H. J. Kbashi, S. V. Sergeyev, M. Al-Araimi, A. Rozhin, D. Korobko, and A. Fotiadi, Opt. Lett. **44**, 5112 (2019).
11. S. A. Kolpakov, H. J. Kbashi, and S. Sergeyev, in Conference on Lasers and Electro-Optics, OSA Technical Digest 2016, (Optical Society of America, 2016)., p. JW2A.56.
12. S. V. Sergeyev et al. In Real-time Measurements, Rogue Events, and Emerging Applications Digest 2016 (International Society for Optics and Photonics, 2016) SPIE, 54 (2016), vol. 9732, p. 97320K.
13. A. F. J. Runge, C. Aguergaray, N. G. R. Broderick, and M. Erkintalo, Opt. Lett. **39**, 319 (2014).
14. D.V. Churkin, O. A. Gorbunov, and S. V. Smirnov, Opt. Lett. **36**, 3617 (2011).
15. S. Randoux, and P. Suret, Opt. Lett. 37, 500 (2012).
16. O. A. Gorbunov, S. Sugavanam, and D. V. Churkin, Opt. Express **22**, 28071 (2014).
17. J. Xu, J. Wu, J. Ye, J. Song, B. Yao, H. Zhang, et al. Photonics Res. **8**, 1-7. (2020).
18. O. A. Gorbunov, S. Sugavanam, I. D. Vatnik, I.D. and D. V. Churkin,. Opt Lett. **45**, 2375 (2020).
19. D. V. Churkin, S. Sugavanam, I. D. Vatik, Z. Wang, E. V. Podivilov, S. A. Babin, et al. Adv. Opt. Photon. **7**, 516 (2015)
20. B. C. Lima, P. I. Pincheira, E. P. Raposo, L. D. S. Menezes, C. B. de Araújo, A. S. Gomes, and R. Kashyap, Phys. Rev. A **96,** 013834 (2017).
21. G. Ansmann, R. Karnatak, K. Lehnertz, and U. Feudel, Phys. Rev. E **8**, 052911 (2013).
22. A. Doutté, P. Suret, and S. Randoux, Opt. Lett. **28**, 2464 (2003).
23. P. Suret, A. Doutté, and S. Randoux, Opt. Lett. **29**, 2166 (2004)

References with titles

1. M. Onorato, S. Residori, U. Bortolozzo, A. Montina, and F. T. Arecchi, "Rogue waves and their generating mechanisms in different physical contexts," Phys. Rep. **528**, 47–89 (2013).
2. N. Akhmediev, B. Kibler, F. Baronio, M. Belić, W. P. Zhong, Y. Zhang, W. Chang, J. M. Soto-Crespo, P. Vouzas, P. Grelu, and C. Lecaplain, "Roadmap on optical rogue waves and extreme events," J Optics **18**, 063001 (2016).
3. H. Kbashi, S. V. Sergeyev, C. Mou, C., A. Martinez, M. A. Araimi, A. Rozhin, S. Kolpakov, and V. Kalashnikov, V., "Bright-Dark Rogue Waves," Ann. Phys. **530**, 1700362. (2018).
4. H. J. Kbashi, S. V. Sergeyev, M. A. Araimi, N. Tarasov, N. and A. Rozhin, A., "Vector soliton rain," Laser Phys. Lett. **16**, 035103 (2019).
5. H. J. Kbashi, M. Zajnulina, A. G. Martinez, S. V. Sergeyev, "Mulitiscale spatiotemporal structures in mode-locked fiber lasers," Laser Phys. Lett. **17**, 035103 (2020).
6. J. M. Dudley, F. Dias, M. Erkintalo, and G. Genty, Instabilities, breathers and rogue waves in optics, Nature Photon. 8, 755-764 (2014)
7. C. Lecaplain, Ph. Grelu, J. M. Soto-Crespo, and N. Akhmediev, Dissipative rogue wave generation in multiple-pulsing mode-locked fiber laser, J. Opt. 15, 064005 (2013).
8. C. Lecaplain, Ph. Grelu, J. M. Soto-Crespo and N. Akhmediev, Dissipative rogue waves generated by chaotic pulse bunching in a mode-locked laser, Phys. Rev. Lett. 108, 233901 (2012).
9. J. M. Soto-Crespo, Ph. Grelu, and N. Akhmediev, Dissipative rogue waves: extreme pulses generated by passively mode-locked lasers.Phys. Rev. E 84, 016604 (2011).
10. H. J. Kbashi, S. V. Sergeyev, M. Al-Araimi, A. Rozhin, D. Korobko, and A. Fotiadi, "High-frequency vector harmonic mode locking driven by acoustic resonances," Opt. Lett. **44**, 5112 (2019).
11. S. A. Kolpakov, H. J. Kbashi, and S. Sergeyev, "Slow Optical Rogue Waves in a Unidirectional Fiber Laser", in Conference on Lasers and Electro-Optics, OSA Technical Digest 2016, (Optical Society of America, 2016)., p. JW2A.56.
12. S. V. Sergeyev , et al. "Slow deterministic vector rogue waves", In Real-time Measurements, Rogue Events, and Emerging Applications Digest 2016 (International Society for Optics and Photonics, 2016) SPIE, 54 (2016), vol. 9732, p. 97320K.
13. A. F. J. Runge, C. Aguergaray, N. G. R. Broderick, and M. Erkintalo, "Raman rogue waves in a partially mode-locked fiber laser," Opt. Lett. 39, 319–322 (2014).
14. D.V. Churkin, O. A. Gorbunov, and S. V. Smirnov, "Extreme value statistics in Raman fiber lasers," Opt. Lett. **36**, 3617 (2011).
15. S. Randoux, and P. Suret, "Experimental evidence of extreme value statistics in Raman fiber lasers," Opt. Lett. **37**, 500 (2012).
16. O. A. Gorbunov, S. Sugavanam, and D. V. Churkin, "Revealing statistical properties of quasi-CW fibre lasers in bandwidth-limited measurements," Opt. Express **22**, 28071 (2014).
17. J. Xu, J. Wu, J. Ye, J. Song, B. Yao, H. Zhang, J. Leng, W. Zhang, P Zhou, and Y. Rao, Optical rogue wave in random fiber laser. Photonics Res. **8**, 1-7. (2020).
18. O. A. Gorbunov, S. Sugavanam, I. D. Vatnik, I.D. and D. V. Churkin,. "Poisson distribution of extreme events in radiation of random distributed feedback fiber laser", Opt Lett. **45**, 2375 (2020).
19. D. V. Churkin, S. Sugavanam, I. D. Vatik, Z. Wang, E. V. Podivilov, S. A. Babin, Y. Rao, and S. K. Turitsyn, "Recent advances in fundamentals and applications of random fiber lasers," Adv. Opt. Photon. **7**, 516–569 (2015).
20. B. C. Lima, P. I. Pincheira, E. P. Raposo, L. D. S. Menezes, C. B. de Araújo, A. S. Gomes, and R. Kashyap, "Extreme-value statistics of intensities in a cw-pumped random fiber laser," Phys. Rev. A **96,** 013834 (2017).
21. G. Ansmann, R. Karnatak, K. Lehnertz, and U. Feudel, Extreme events in excitable systems and mechanisms of their generation, Phys. Rev. E **8**, 052911 (2013).
22. A. Doutté, P. Suret, and S. Randoux, "Influence of light polarization on dynamics of continuous-wave-pumped Raman fiber lasers," Opt. Lett. **28**, 2464 (2003).
23. P. Suret, A. Doutté, and S. Randoux, "Influence of light polarization on dynamics of all-fiber Raman lasers: theoretical analysis," Opt. Lett. **29**, 2166 (2004).